

Integrated electric vehicle design and simulation: Combining a mechanical and electrical model using Simscape/Multibody

Hatim Jbari, Rachid Askour, Badr Bououlid Idrissi

Modeling Information Processing and Control Systems (MPICS), National High School of Arts and Crafts,
Moulay Ismail University, Meknes, Morocco

Article Info

Article history:

Received May 12, 2024

Revised Aug 19, 2024

Accepted Sep 5, 2024

Keywords:

Electric vehicle

Hybrid energy storage system

PID control

Simscape/Multibody

Supercapacitors

ABSTRACT

This paper presents a novel methodology for modeling and implementing an electric vehicle (EV) simulation model using the Multibody approach. The proposed method provides a robust solution for studying EV performance, taking into consideration the dynamic behavior of its complex mechanical system. The mechanical design was carried out using SOLIDWORKS software and then exported to the Simscape/Multibody platform. This process was performed to combine the obtained mechanical design with an electrical model, developed using the Simscape and MATLAB/Simulink toolbox, in the same simulation platform. The proposed EV is powered by an electromechanical PowerDrive based on a permanent magnet synchronous machine (PMSM), supplied by a hybrid energy storage system (HESS). The implemented HESS, operating in a fully active topology, is controlled by a deterministic rule-based energy management system (EMS). To evaluate the proposed model performance, simulations were conducted under ECE-15.

This is an open access article under the [CC BY-SA](https://creativecommons.org/licenses/by-sa/4.0/) license.



Corresponding Author:

Hatim Jbari

Modeling Information Processing and Control Systems (MPICS), National High School of Arts and Crafts

Moulay Ismail University

B.P. 15290 EL Mansour Meknes 50500, Meknes, Morocco

Email: ha.jbari@edu.umi.ac.ma

1. INTRODUCTION

Today, research and development investments are predominantly made by the automotive industry to create more efficient, safer, and more competitive vehicles. This field is also challenged by increasingly stringent environmental and safety regulations [1]-[3]. Consequently, this situation requires technological advancements like engine electrification and the incorporation of ecologically friendly transportation options, such as electric vehicles (EV) [4]-[6]. However, the complex process involved in EV design depends on various factors, including performance aspects like range, stability, and durability, as well as the design methodologies and tools used to manage the complex interactions between components [7], [8].

According to the literature, several studies have been conducted in the field of complex system design, specifically focusing on dynamics and control. A recent study [9] introduced a three-dimensional dynamic model of an 8x8 nonlinear wheeled vehicle, developed using the "Universal Mechanism" software for Multibody system simulations, and included a MATLAB/Simulink model of tire-terrain interaction. This work aims to evaluate the vehicle's dynamic behavior and stability during acceleration and braking. Another work [10] has presented a control model using model predictive control (MPC) for the lateral dynamics of a four-wheel drive vehicle. The authors used the ADAMS-Car platform for mechanical modeling, and MATLAB for integrating state space representation with the control model. The primary objective of this study was to enhance vehicle handling by controlling wheel torque. Preview study [11], a simplified vehicle simulation

model was developed using the ADAMS platform to compare suspension dynamics with real terrain experimental results, aiming to identify mismatches between simulation and real data. Preview study [12], a two-wheeled unmanned ground vehicle (UGV) using a Multibody approach is introduced. The proposed vehicle integrates a trajectory-tracking motion control, based on extended Kalman filter, and realistic Simscape/Multibody simulations. Recent work in [13] details a Multibody-based eight-legged robot, focusing on validating fuzzy controllers for optimal joint control while considering the system's interactions with its environment.

In the same context, several partners, researchers, and industrial professionals working on land mobility, aim to overcome EV challenges by developing new architectures and algorithms [14]-[18]. Their objective is to enhance EV performance and overcome various challenges including limited range and battery lifespan [19]-[21]. Indeed, a recent work in [22] introduced a 30kW semi-active hybrid energy storage system (HESS) for an EV, based on batteries and supercapacitors (SC). The system uses a fuzzy logic controller (FLC) based EMS for real-time control and power filtering. This work aims to improve efficiency and battery lifespan by minimizing current peaks and voltage drops. Furthermore, the authors in [23], [24] present EV models powered by a HESS using the energetic macroscopic representation (EMR) approach. These studies aim to enhance the performance of the proposed architecture through the SC integration and the implementation of an FLC-based EMS, consequently improving the battery's lifespan.

This article presents a simulation of a 5 kW EV model, based on a multibody approach. The mechanical model was developed on SOLIDWORKS and imported into the Simscape/Multibody platform. The electrical machine based on the permanent magnet synchronous machine (PMSM) and the HESS, were developed using Simulink and Simscape toolbox. The HESS is controlled by a deterministic rule-based EMS, which was designed to optimize energy flow. This work aims to evaluate the proposed EV model for more realistic simulations, and EMS performance, considering the complexity of the mechanical parts. The structure of the proposed paper is as: i) section 2 presents the proposed modeling and control of the EV, ii) section 3 describes the EV power management system in detail, iii) section 4 presents simulation results and discussions, and iv) section 5 presents the conclusion of the paper.

2. EV SYSTEM MODELING AND CONTROL

2.1. Description of the studied EV

The studied system is a single-seat EV with a maximum speed of 50 km/h, designed for intra-city transportation and goods delivery. The EV is driven by a 5kW PMSM, supported by a fully active HESS. The designed HESS includes a Li-Ion battery and supercapacitors, combined with two DC-DC converters as shown in Figure 1.

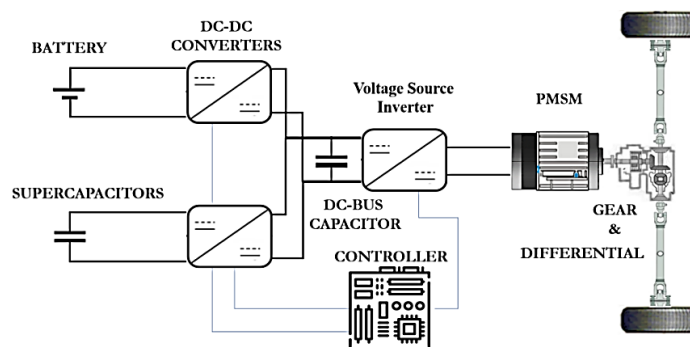


Figure 1. Simplified block diagram of the EV powertrain

2.2. Mechanical model

The EV multi-body simulation model was constructed in the SOLIDWORKS computer-aided design (CAD) environment. Assembly constraints were meticulously applied to maintain the structural integrity of the system and to define the material properties of each component. The mechanical design of the proposed EV includes various elements that are essential for its interaction with the road, including mainly dampers, upper and lower control arms (wishbones), knuckles, wheel discs, universal joints, rims, and tire, as illustrated in Figure 2. Indeed, the designed vehicle has a total mass of $m_{veh} = 280$ kg and an aerodynamic standard of $C_x S = 0.7$ m².

Once the EV CAD file is finalized, it can be exported in “.XML” format containing the mechanical characteristics and constraints in “.STEP” format, then imported into MATLAB to construct the Simscape/Multibody model. After verifying the model’s integrity, the Simscape blocks are organized and the terrain is integrated to interact with the wheels, as is shown in Figure 3. The Simscape/Multibody block diagram of the PMSM shaft, shown in Figure 4, includes the "Revolute1" block, which represents the mechanical linkage between the motor frame and its shaft. This block is configured with torque 'T' as input and speed 'W' as output, enabling the integration of mechanical and electrical environments through the PMSM.

In system control, the integral proportional (IP) controller is used to maintain the desired vehicle speed, by adjusting the PMSM's parameters based on the difference between the ECE-15 speed reference and EV speed. This adjustment uses IP feedback to optimize the traction force, as in (1). The model operates as a second-order system described by a linear differential equation with constant coefficients. The IP controller gains, K_I and K_P , are theoretically determined to meet stability, accuracy, and speed of response requirements, ensuring a closed-loop control system with a damping coefficient of $m = 0.7$, prioritizing control system speed.

$$F_{veh_tr} = (v_{ev_ref} - v_{ev_meas}).C_c(t) + F_{env_meas} \quad (1)$$

2.3. PowerDrive model

In this study, the power drive is assured by a PMSM, controlled by a three-phase VSI. The adopted VSI architecture is based on insulated gate bipolar transistors (IGBTs) as illustrated in Figure 5. The specific characteristics of the PMSM used in this configuration are illustrated in Table 1.

Table 1. PMSM characteristics

| Parameter | Value |
|-------------------------|----------------------|
| Nominal power | $P_n = 5 \text{ kW}$ |
| L_d inductance | 5.65 mH |
| L_q inductance | 7.50 mH |
| Stator resistance R_s | 0.22Ω |
| Permanent magnet flux | 0.31 wb |

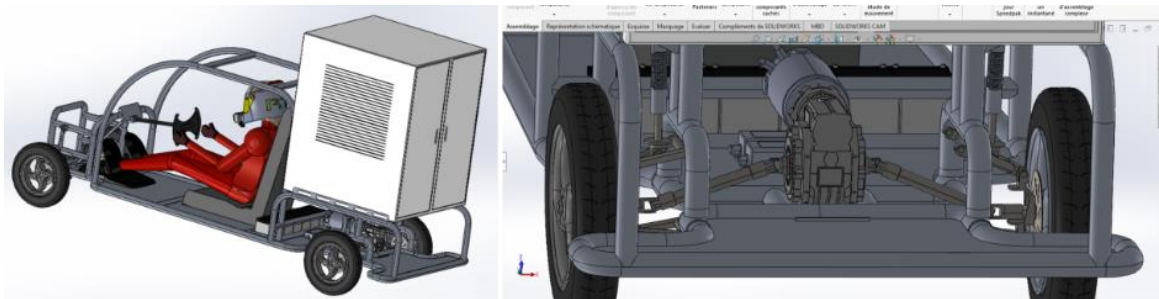


Figure 2. EV SOLIDWORKS CAD model

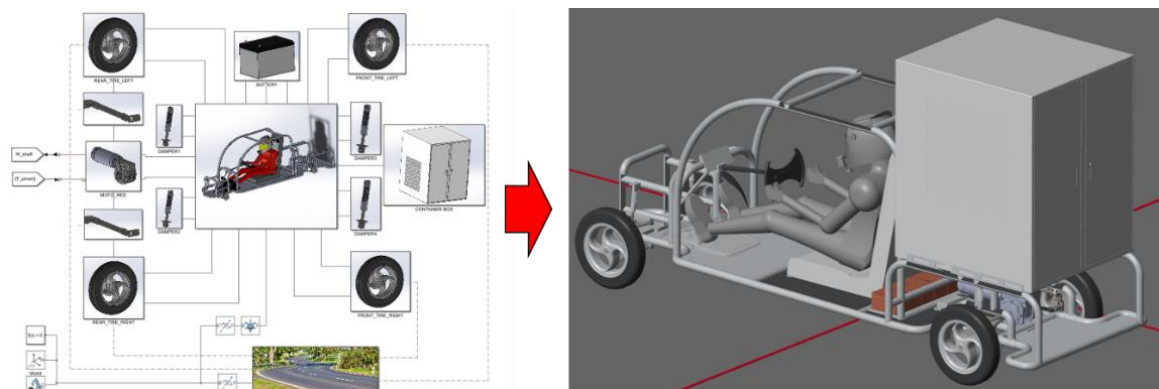


Figure 3. Simscape/Multibody model simulation platform ran in mechanics explorer

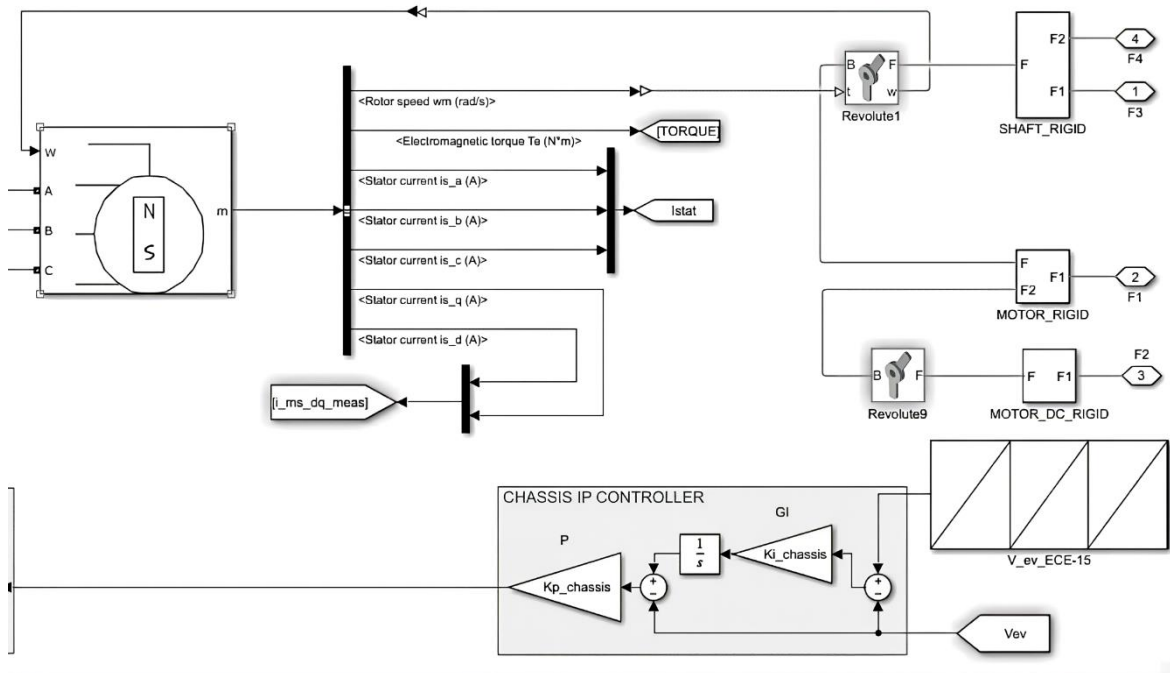


Figure 4. Simscape/Multibody block diagram of the PMSM shaft and mechanical IP controller

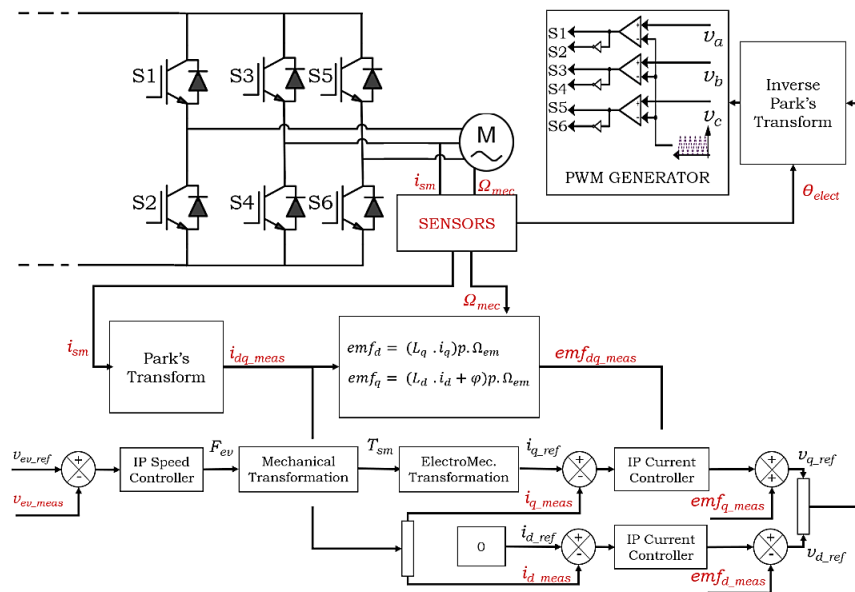


Figure 5. Simscape/Multibody model of the PMSM PowerDrive

The approach adopted in this research is based on simplified models of the electromechanical system. The analytical framework is defined by several key equations: as in (2) describes the relationship between (speed, traction force) and (wheels speed, mechanical torque). Subsequently, (3) establishes the relationship between torque and speed output of the gearbox and the electric machine, incorporating the reduction ratio k_{gear} . Finally, (4) correlates the torque and rotational speed with the currents and voltages of the machine, providing a foundation for detailed analysis of the control and performance of the electric PowerDrive system.

$$\begin{cases} T_{gear} = R_{wheel} \cdot F_{veh_tr} \\ v_{ev} = R_{wheel} \cdot \Omega_{gear} \end{cases} \quad (2)$$

$$\begin{cases} T_{em} = \eta_{eff} \cdot r_{gear} \cdot T_{gear} \\ \Omega_{gear} = \eta_{eff} \cdot r_{gear} \cdot \Omega_{em} \end{cases} \quad (3)$$

$$\begin{cases} T_{em} = \frac{3}{2} p [\varphi_v i_q + (L_q - L_d) i_q \cdot i_d] = k \cdot \varphi \cdot i_q \\ e_{dq} = f(i_{dq}, \theta_{elect}, \varphi, \Omega_{em}) \end{cases} \quad (4)$$

In this study, the maximum torque per ampere (MTPA) was adopted. It controls the PMSM by adjusting torque based on the electrical current i_q as demonstrated in (5). This method minimizes power losses by setting the i_d current to zero when the machine operates below base speed. The control of inductance voltages in the PMSM requires two IP controllers to generate reference voltages U_{dq_ref} (6). The inverse Park transformation (7) converts U_{dq_ref} to U_{sm_ref} for generating pulse width modulation (PWM) signals. These signals control the IGBTs and coordinate the PMSM's three-phase voltage by comparing a triangular signal with U_{sm_ref} , as detailed in Figure 5, to produce correct switching sequences.

$$i_q = \frac{2T_{em}}{3p[\varphi_v + (L_q - L_d)i_d]} \quad (5)$$

$$U_{dq_ref} = (i_{dq_ref} - i_{dq_meas}) \cdot C_S(t) + e_{dq_meas} \quad (6)$$

$$U_{sm_ref} = [P(\theta_{elect})]^{-1} U_{dq_ref} \quad (7)$$

2.4. HESS electrical model

The proposed vehicle in this work combines an electric propulsion system and an onboard energy storage system. One of the main objectives of this study is to design a HESS that combines batteries and SC. The complementarity between these energy sources allows the improvement of the global performance of the system. Indeed, the adopted architecture is that of a full-active topology HESS with two parallel DC-DC converters as it is illustrated in Figure 6.

The first part of the used DC-DC converter is represented by the current smoothing inductors. According to (8), inductance and internal resistance (L_{source} , r_{source}) are considered as the main characteristics.

$$\begin{cases} L_{bat} \frac{d}{dt} i_{bat} = U_{bat} + U_{L_bat} + r_{L_bat} i_{bat} \\ L_{SC} \frac{d}{dt} i_{SC} = U_{SC} + U_{L_SC} + r_{L_SC} i_{SC} \end{cases} \quad (8)$$

The smoothing inductors L_{bat} and L_{SC} are used to limit the current ripple Δi_{Batt} at the input of the converter. Since the converters are identical, the values of the L_{bat} and L_{SC} inductances are the same, as in (9).

$$L_{bat} = L_{SC} > \frac{U_{DC}}{4.f.\Delta i_{bat}} \quad (9)$$

On the other hand, the DC-DC converters, are of bidirectional type, each containing four semiconductors: two MOSFET and two free-wheeling diodes. The MOSFETs switch between the ON and OFF states to ensure the power transfer from both sources in boost-buck mode. Thus, the switching model is presented in (10) and (11), where α_{bat} and α_{sc} represent the duty cycles of the converters, η_{ch_bat} , and η_{ch_bat} represent respectively the DC-DC converter's efficiencies.

$$\begin{cases} U_{L_bat} = \alpha_{bat} \cdot U_{DC} \\ i_{ch_bat} = \eta_{ch_bat} \cdot \alpha_{bat} \cdot i_{bat} \end{cases} \quad (10)$$

$$\begin{cases} U_{L_SC} = \alpha_{SC} \cdot U_{DC} \\ i_{ch_SC} = \eta_{ch_SC} \cdot \alpha_{SC} \cdot i_{SC} \end{cases} \quad (11)$$

On the other hand, the implemented filter capacitor is used to ensure a continuous supply at the output of the HESS voltage, to limit the DC bus voltage ripple, as defined in (12).

$$C \frac{d}{dt} U_{DC} = i_{hess} - i_{DC} \quad (12)$$

The C capacitor is defined in (13).

$$C > \frac{i_{DC}}{4 \cdot f \cdot \Delta U_{DC}} \quad (13)$$

Indeed, the implementation of local control should make it possible to keep the DC bus voltage (U_{DC}) constant by controlling the appropriate current values, taking into account the contribution of each source (battery, SC). A power-sharing technique is implemented to meet the requirements of the driving profile. Thus, a first IP controller is used to control the main HESS voltage (U_{DC}), this controller supports a constant voltage reference $U_{DC} = 220$ V defined by the EMS and allows to determine the value of the main reference current: i_{hess_ref} for both sources as described in (14).

$$C \frac{d}{dt} U_{DC} = i_{hess} - i_{DC} \quad (14)$$

The control scheme shown in Figure 6 describes the architecture used for this mode of operation. Two current control loops are implemented for (15) and (16), where the battery reference current is defined from the EMS to determine the contribution of this source according to the driving cycle phases. Whereas the reference current of the SC is derived from the node law (17). This control scheme makes it possible to determine the voltages required for the duty cycle calculation (α_{bat} and α_{sc}), which control the DC-DC converter switches. This is carried out to satisfy the DC bus requirements of the U_{DC} voltage stability and the main current i_{DC} demanded by the PowerDrive system.

$$U_{L_bat_ref} = (i_{bat_ref} - i_{bat_meas}) \cdot C_c(t) + U_{bat_meas} \quad (15)$$

$$U_{L_SC_ref} = (i_{SC_ref} - i_{SC_meas}) \cdot C_c(t) + U_{SC_meas} \quad (16)$$

$$i_{hess} = i_{ch_SC} + i_{ch_bat} \quad (17)$$

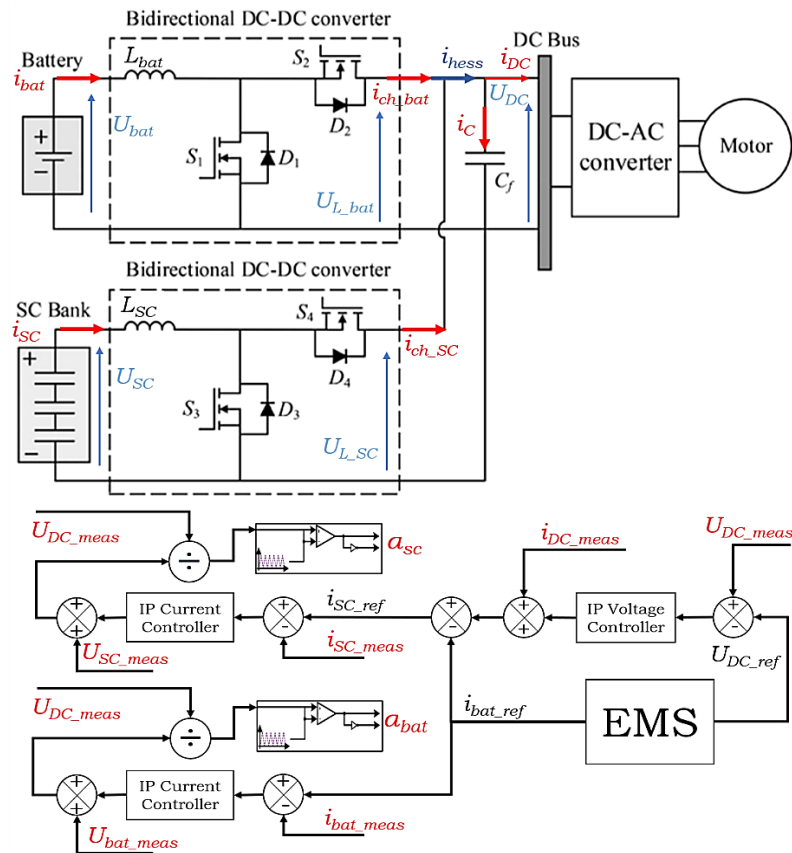


Figure 6. Simscape/Multibody model of the EV HESS

3. ENERGY MANAGEMENT SYSTEM

Multi-source storage systems are increasingly being used in electric mobility, to support the energy needs of EVs. These systems, particularly those based on batteries and SCs, combine the advantages of both technologies. The SCs integration provides high power for short periods, while batteries ensure energy supply over long periods for quasi-static power demands.

In order to define the contribution of both energy sources, EMS takes into account several factors, such as the state of charge of the battery and the SCs, the driving cycle profile, and the minimization of battery stress. Indeed, a deterministic rule-based EMS has been developed to ensure control of energy flow between the powertrain and the HESS energy sources [25]. The proposed EMS scheme, described in Figure 7, uses an algorithm that takes as inputs: the EV speed v_{veh} and the acceleration A_{veh} to define the driving phase of the vehicle, the SoC_{SC} , and the SoC_{bat} to check the availability of energy in both sources, the values of the U_{DC} voltage, the currents I_{DC} and I_{SC} to define the power reference. The primary objective of the designed EMS is to keep the DC bus voltage constant, using the battery for steady-state power supply and the SCs for transient power supply, more specifically high and fast power demands.

This principle makes it possible to minimize the load on the battery and improve its lifespan while still providing the powertrain required power. The various scenarios that can be studied are therefore shown in the flowchart in Figure 8, and the operating mode of the EMS is described as follows:

- a) Traction phase: refers to the phase when the vehicle is operating in traction mode, where the storage is supposed to provide energy. Two situations are possible during this cycle:
 - Acceleration phase ($A_{veh} > 0$ & $v_{veh} > 0$): when the load power demand is higher than the battery power limit. The EMS should check if the SoC_{SC} is allowing the SCs to produce energy. In this case, the battery and the SCs generate the required power. Thus, fast power demands should be supported by the SCs, as these are characterized by fast dynamics, the battery should be progressively engaged to compensate for the remaining power. On the other hand, if the SCs are not available ($SoC_{SC} < SoC_{SC_min} = 50\%$) [17], the EMS stops discharging the SCs and the battery provides the entire required power.
 - Constant and quasi-constant speed phase ($A_{veh} = 0$ & $v_{veh} > 0$): when the load power demand is constant and the SoC_{bat} is available on the battery packs, it takes over the power supply to the powertrain. The difference in power is used to charge the SCs using (18). The SCs are therefore charged until the stop charge condition is reached: $SoC_{SC}(t) > SoC_{SC_init} = 95\%$.

$$P_{bat_ref} = f(SoC_{SC}) = P_{max} \cdot \left(\frac{SoC_{SC_init} - SoC_{SC}(t)}{100} \right) \quad (18)$$

- b) Decelerating and braking: during this cycle, the kinetic energy generated during deceleration is converted into electrical energy regenerated by the PMSM. The reverse torque observed during braking is caused by the electromotive force (EMF) induced in the machine, which then creates a reverse current in the DC bus. This process produces very high magnitude and short-duration power pulses in the HESS. Indeed, the SC are prioritized for recharging to support high power pulses and then to increase their availability to restore them to the initial state of charge ($SoC_{SC}(t) = SoC_{SC_init} = 95\%$), enabling a power buffer function.
- c) EV total stop phase: During this period, the EMS should check the SoC_{SC} by comparing it to ($SoC_{SC_init} = 95\%$). If this condition is not met ($SoC_{SC}(t) < SoC_{SC_init}$), the EMS should progressively engage the battery to charge the SCs according to (19) to restore them to their SoC_{SC_init} . In this case, the HESS architecture and the implemented control should allow the interchangeability of the energy flow between the used sources.

$$P_{bat_ref} = f(I_{SC}) = U_{DC_meas} \cdot I_{SC} \quad (19)$$

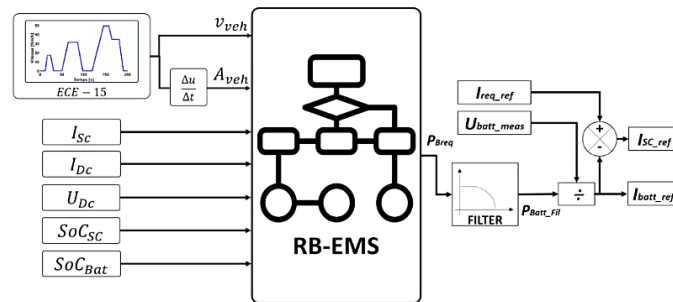


Figure 7. Block diagram of the proposed EV EMS

The designed EMS integrates a low-pass filter to split required power reference into a high-frequency signal supported by the (SCs), and a low-frequency signal designed to be supplied by the battery. This configuration reduces the high-frequency power demand variations that can impact battery performance.

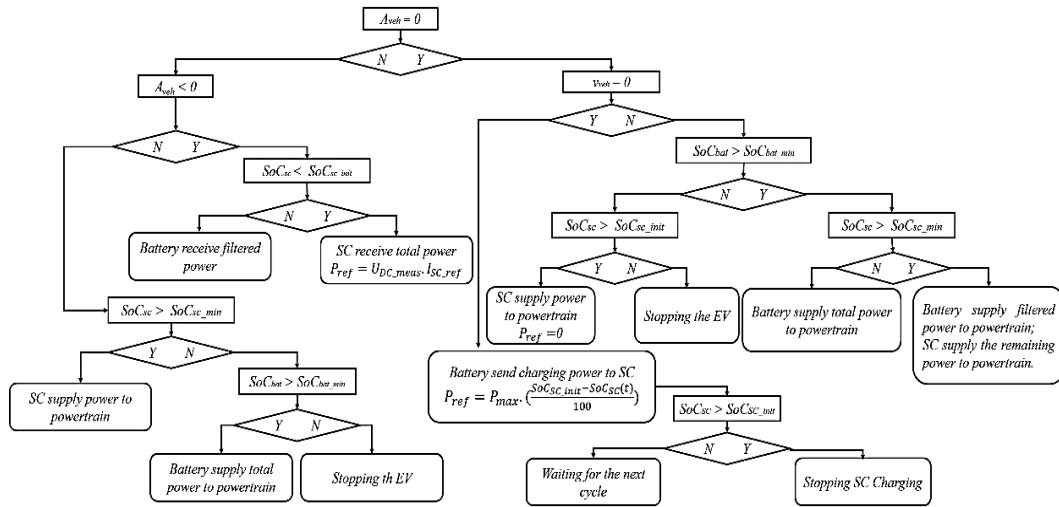


Figure 8. Flowchart of the proposed EMS algorithm

4. RESULTS AND DISCUSSION

The EV model was constructed on MATLAB using Simscape library. The control and the EMS were organized into subsystems on the same platform, as shown in Figure 9. The coupling between the PMSM and the mechanical model was performed through the "Revolute" block of the motor gearbox shaft. The evaluation of the simulation model is performed using MATLAB/Simulink under the ECE-15 with a sampling time of 10^{-6} . Table 2 and Table 3 show the battery and SC characteristics respectively.

Therefore, the analysis of the energy parameter curves shown in Figure 10, which reflect the performance of the EV powertrain, highlights several important observations. Firstly, the comparison of the vehicle speed response with the setpoint generated by the ECE-15 profile, shows that the response follows the setpoint during acceleration, constant speed, deceleration, and braking. The obtained results demonstrate the appropriate choice of IP controller parameters, particularly their ability to minimize overshoot and ensure acceptable accuracy. The IP controllers meet the requirements of the vehicle design optimally. In addition, the torque generated by the PMSM is proportional to the speed variation of the vehicle. The stator currents I_{abc} are sine-shaped with slight ripple due to the selected PWM frequency of 20 kHz.

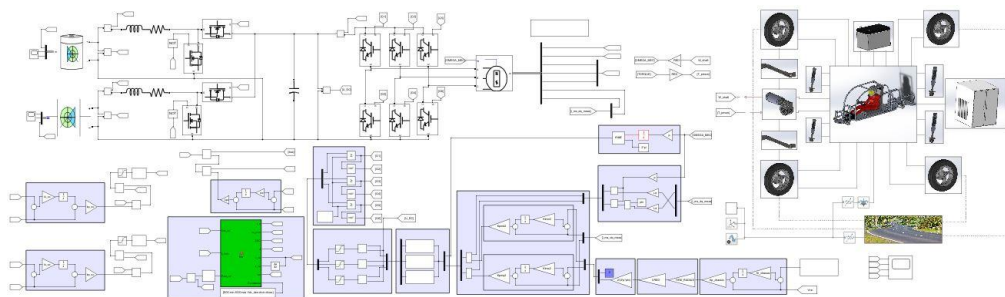


Figure 9. Simulation model of the proposed system

Moreover, Figure 11 illustrates the variation of HESS parameters throughout the ECE-15 driving cycle. The analysis of the curve patterns demonstrates that the SoC_{SC} has variations in accordance with the machine power demand variations, taking into account the range defined in the EMS design $SoC_{SC} \in [50, 100]\%$ to ensure SCs optimal energy performance. While SoC_{bat} is generally smoothed and shows low variation,

minimizing battery stress and thus optimizing battery life. Furthermore, the power profile of the powertrain shows variations that depend on the driving phases of the vehicle, with a maximum power value of $P_{dem_max} = 3$ kW. A key criterion in assessing the robustness of an EMS is the DC-bus voltage stability. Indeed, the profile of this parameter illustrated in Figure 11 is constant with slight variations that remain below $\Delta U_{DC} = 3$ V, demonstrating the reliability of the EMS algorithm and the control implemented in the HESS.

Table 2. Li-Ion battery characteristics (3.7V LI-CELLS) Table 3. Supercapacitors characteristics (GTCAP 2.7V)

| Parameter | Value |
|------------------------------------|------------|
| SoC limits | [30, 100]% |
| SoC _{bat_init} | 96% |
| Number of cells in series-parallel | 40-29 |
| Nominal voltage | 148 V |
| Cell capacity | 3.8 Ah |
| Battery capacity | 110 Ah |
| Power limit | 5 kW |

| Parameter | Value |
|------------------------------------|------------|
| SoC limits | [50, 100]% |
| SoC _{SC_init} | 97% |
| Nominal voltage | 148.5 V |
| Cells number in series | 55 |
| Equivalent series resistance (ESR) | 0.21 mΩ |
| SCs cell capacitance | 1500 F |

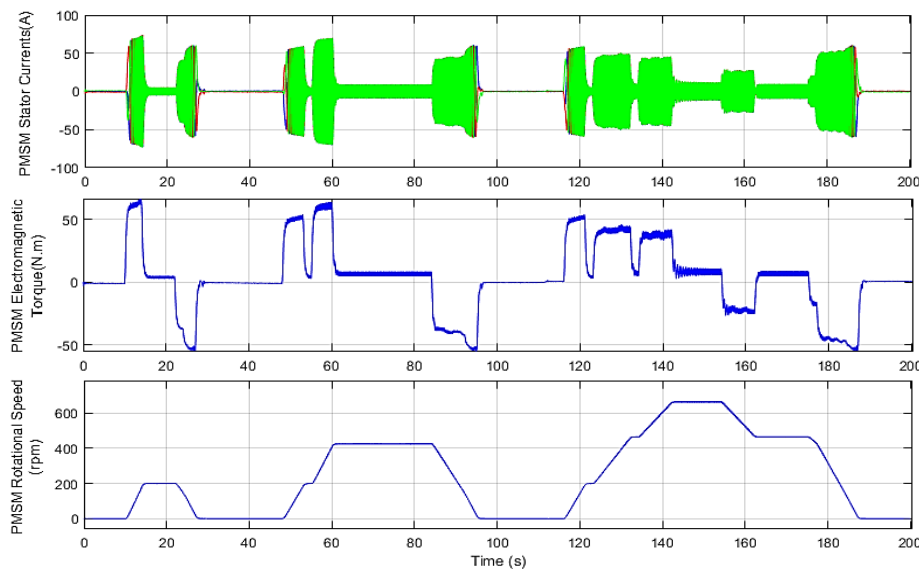


Figure 10. Simulation results (PMSM stator currents, electromagnetic torque, and rotational speed)

- Acceleration cycle: $t \in [10, 15]$ s, $t \in [50, 60]$ s and $t \in [118, 143]$ s: The EV speed response gradually increases following the ECE-15 speed setpoint, as both parameters are in perfect agreement, resulting in a tracking error of $\varepsilon_{tr_ve} = 0.36$ km/h. During this period, the machine receives maximum current reaching 75A in [12, 15] s time interval as shown in Figure 10, developing maximum torque of 69 N.m at a machine speed of $\Omega_{em} = 200$ rpm to reach $v_{veh} = 15.7$ km/h. According to the mechanical explorer visualization on the Simscape/Multibody platform, the torque of the PMSM was able to overcome all the resisting torques due to the vehicle's rolling torque and rotating mass inertia. On the other hand, the fast decrease of the SoC_{SC} , shown in the curve of Figure 11, reaching a value of $SoC_{SC} = 95\%$ at $t = 2$ s, shows that the SCs are activated by EMS to satisfy the high powers demanded by the PMSM, while the SoC_{bat} shows a low decrease, providing a progressive power contribution to support the following cycle.
- Stabilized speed cycle: $t \in [15, 23]$ s, $t \in [60, 85]$ s, $t \in [143, 155]$ s and $t \in [163, 176]$ s: The EV speed still follows the reference speed, stabilizing at different speeds of $v_{veh} = 12$ km/h at $t \in [15, 23]$ s, $v_{veh} = 27$ km/h at $t \in [60, 85]$ s and $v_{veh} = 48$ km/h at $t \in [143, 155]$ s, with a maximum static error of $\varepsilon_{st_ve} = 0.15$ km/h, and an acceptable maximum overshoot of 0.15% at $t = 40$ s as shown in Figure 10. During this phase, the machine receives a current of stable amplitude, lower than the starting current, with a maximum value of 10 A during [145, 150] s. Meanwhile, the torque decreases progressively and remains constant at a value of 10 N/m for a machine speed of $\Omega_{em} = 200$ rpm. In addition, Figure 11 shows a quasi-constant evolution of the SoC_{SC} and a faster decrease of the SoC_{bat} . Where the EMS activates the battery to support the constant and quasi-constant power demand of the powertrain as shown in Figure 11.
- Deceleration/braking cycle: $t \in [23, 27]$ s, $t \in [85, 96]$ s, $t \in [155, 163]$ s and $t \in [176, 188]$ s : The EV speed decreases progressively in perfect agreement with the setpoint, with a tracking error of $\varepsilon_{tr_ve} = 0.36$ km/h.

During vehicle deceleration and braking, the electromagnetic force (EMF) produced by the PMSM generates a reversed electric current compared to the normal operating current of the machine, which also induces a reversed electromagnetic torque with a maximum value of -60 N.m. This means that the electrical torque generated during braking opposes the vehicle's progress, providing an effective means of decelerating and stopping the vehicle. Simultaneously, this reverse current is used to supply the vehicle's energy storage, optimizing its autonomy.

- Vehicle total stop: $t \in [27, 50]$ s, $t \in [96, 118]$ s, $t \in [188, 200]$: According to Figure 11 the curves show an increase in SoC_{SC} to reach SoC_{SC_init} and stabilize thereafter, at the same time a very small decrease in SoC_{bat} is noticed. Figure 12 shows that the battery current increases progressively, while the SCs current increases with a negative value. This demonstrates that the decisions taken by the EMS are perfectly in accordance with the requirements defined in the algorithm described in Figure 8. Thus, during this phase, the EMS checks that $SoC_{SC} < SoC_{SC_init}$ to engage the battery to restore the SCs to their initial state of charge (energy buffer). In addition, the negative value of the SCs current and the positive value of the battery shown in the curve of Figure 12, demonstrate more clearly this decision taken by the EMS and the energy exchange possibility between sources.

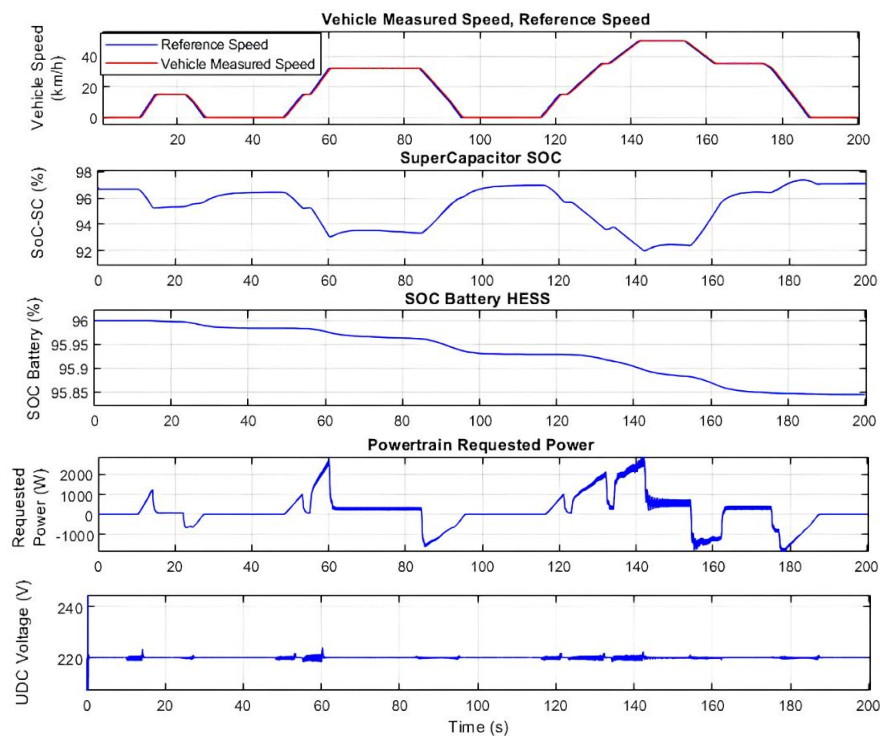


Figure 11. Simulation model results (vehicle speed, SoCs, requested power, U_{DC} voltage)

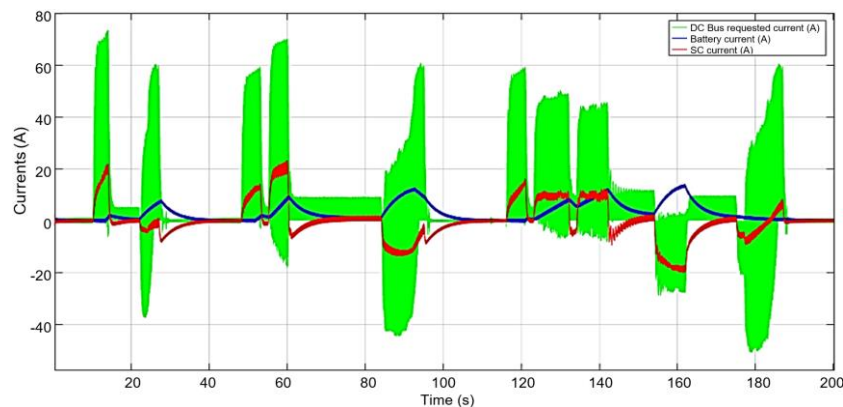


Figure 12. Simulation model results (HESS and sources currents)

5. CONCLUSION

In summary, this work presents an implementation and validation of an EV model based on multibody approach. The proposed simulation model was designed to combine the multibody approach of the vehicle mechanical model, the PowerDrive system built with Simscape blocks, and the control model with the EMS built using MATLAB/Simulink. Indeed, the simulation model of the proposed EV, based on Simscape/Multibody has enabled to offer a realistic simulation of complex multibody systems with fast modeling, taking into account factors such as geometry, kinematics, and dynamics of the EV components, which allows a more accurate analysis of the system. In addition, the study has opted for a more complex architecture on the structural level of the energy conversion system, enables implementation and a more detailed analysis of the system's performance. The role of each power electronics component has been defined during the design of the power converters, implemented in the powertrain and the HESS of the proposed system. Thus, this work has contributed in the optimization of the HESS coupling of SCs with a lithium-ion battery to supply the EV. The sources complementarity allowed the improvement of the global performance of the energy storage system by reducing the solicitations on the battery. Future research will focus on the same model, with greater emphasis on analyzing the dynamics of the proposed electric vehicle (EV) under various driving scenarios, including uphill and downhill driving, as well as cornering.




REFERENCES

- [1] B. L. Salvi and K. A. Subramanian, "Sustainable development of road transportation sector using hydrogen energy system," *Renewable and Sustainable Energy Reviews*, vol. 51, pp. 1132–1155, Nov. 2015, doi: 10.1016/j.rser.2015.07.030.
- [2] D. D. Wang, "Assessing road transport sustainability by combining environmental impacts and safety concerns," *Transportation Research Part D: Transport and Environment*, vol. 77, pp. 212–223, Dec. 2019, doi: 10.1016/j.trd.2019.10.022.
- [3] B. Othman, G. De Nunzio, D. Di Domenico, and C. Canudas-de-Wit, "Ecological traffic management: A review of the modeling and control strategies for improving environmental sustainability of road transportation," *Annual Reviews in Control*, vol. 48, pp. 292–311, 2019, doi: 10.1016/j.arcontrol.2019.09.003.
- [4] M. Bharathidasan, V. Indragandhi, V. Suresh, M. Jasiński, and Z. Leonowicz, "A review on electric vehicle: Technologies, energy trading, and cyber security," *Energy Reports*, vol. 8, pp. 9662–9685, Nov. 2022, doi: 10.1016/j.egyr.2022.07.145.
- [5] G. Pasaoglu, G. Harrison, L. Jones, A. Hill, A. Beaudet, and C. Thiel, "A system dynamics based market agent model simulating future powertrain technology transition: Scenarios in the EU light duty vehicle road transport sector," *Technological Forecasting and Social Change*, vol. 104, pp. 133–146, Mar. 2016, doi: 10.1016/j.techfore.2015.11.028.
- [6] A. Ajanovic and R. Haas, "Dissemination of electric vehicles in urban areas: Major factors for success," *Energy*, vol. 115, pp. 1451–1458, Nov. 2016, doi: 10.1016/j.energy.2016.05.040.
- [7] I. Husain *et al.*, "Electric drive technology trends, challenges, and opportunities for future electric vehicles," *Proceedings of the IEEE*, vol. 109, no. 6, pp. 1039–1059, Jun. 2021, doi: 10.1109/JPROC.2020.3046112.
- [8] J. A. Sanguesa, V. Torres-Sanz, P. Garrido, F. J. Martinez, and J. M. Marquez-Barja, "A review on electric vehicles: technologies and challenges," *Smart Cities*, vol. 4, no. 1, pp. 372–404, Mar. 2021, doi: 10.3390/smartcities4010022.
- [9] V. A. Gorelov, A. I. Komissarov, and A. V. Miroshnichenko, "8×8 wheeled vehicle modeling in a multibody dynamics simulation software," *Procedia Engineering*, vol. 129, pp. 300–307, 2015, doi: 10.1016/j.proeng.2015.12.066.
- [10] H. Kanchwala and C. Bordons, "Improving handling performance of an electric vehicle using model predictive control," in *The 11th International Conference on Automotive Engineering*, Mar. 2015, p. 10. doi: 10.4271/2015-01-0082.
- [11] H. Kanchwala and A. Chatterjee, "ADAMS model validation for an all-terrain vehicle using test track data," *Advances in Mechanical Engineering*, vol. 11, no. 7, p. 168781401985978, Jul. 2019, doi: 10.1177/1687814019859784.
- [12] R. Carbonell, A. Cuenca, V. Casanova, R. Pizá, and J. J. Salt Llobregat, "Dual-rate extended Kalman filter based path-following motion control for an unmanned ground vehicle: realistic simulation," *Sensors*, vol. 21, no. 22, p. 7557, Nov. 2021, doi: 10.3390/s21227557.
- [13] A. A. Aldair, A. Al-Mayyahi, and B. H. Jasim, "Control of eight-leg walking robot using fuzzy technique based on SimScape Multibody toolbox," *IOP Conference Series: Materials Science and Engineering*, vol. 745, no. 1, p. 012015, Feb. 2020, doi: 10.1088/1757-899X/745/1/012015.
- [14] S. Chakraborty *et al.*, "Embedded systems and software challenges in electric vehicles," in *2012 Design, Automation & Test in Europe Conference & Exhibition (DATE)*, IEEE, Mar. 2012, pp. 424–429. doi: 10.1109/DATE.2012.6176508.
- [15] M. S. H. Lipu *et al.*, "Artificial intelligence approaches for advanced battery management system in electric vehicle applications: A statistical analysis towards future research opportunities," *Vehicles*, vol. 6, no. 1, pp. 22–70, Dec. 2023, doi: 10.3390/vehicles6010002.
- [16] Z. Li, A. Khajepour, and J. Song, "A comprehensive review of the key technologies for pure electric vehicles," *Energy*, vol. 182, pp. 824–839, Sep. 2019, doi: 10.1016/j.energy.2019.06.077.
- [17] F. Un-Noor, S. Padmanaban, L. Mihet-Popa, M. Mollah, and E. Hossain, "A comprehensive study of key electric vehicle (EV) components, technologies, challenges, impacts, and future direction of development," *Energies*, vol. 10, no. 8, p. 1217, Aug. 2017, doi: 10.3390/en10081217.
- [18] S. Pareek, A. Sujil, S. Ratra, and R. Kumar, "Electric vehicle charging station challenges and opportunities: a future perspective," in *2020 International Conference on Emerging Trends in Communication, Control and Computing (ICONC3)*, IEEE, Feb. 2020, pp. 1–6. doi: 10.1109/ICONC345789.2020.9117473.
- [19] V. M. Macharia, V. K. Garg, and D. Kumar, "A review of electric vehicle technology: Architectures, battery technology and its management system, relevant standards, application of artificial intelligence, cyber security, and interoperability challenges," *IET Electrical Systems in Transportation*, vol. 13, no. 2, p. e12083, Jun. 2023, doi: 10.1049/els2.12083.
- [20] A. Ghosh, "Possibilities and challenges for the inclusion of the electric vehicle (EV) to reduce the carbon footprint in the transport sector: a review," *Energies*, vol. 13, no. 10, p. 2602, May 2020, doi: 10.3390/en13102602.
- [21] X. Liu, F. Zhao, H. Hao, and Z. Liu, "Opportunities, challenges and strategies for developing electric vehicle energy storage systems under the carbon neutrality goal," *World Electric Vehicle Journal*, vol. 14, no. 7, p. 170, Jun. 2023, doi: 10.3390/wevj14070170.




- [22] Q. Zhang and G. Li, "Experimental study on a semi-active battery-supercapacitor hybrid energy storage system for electric vehicle application," *IEEE Transactions on Power Electronics*, vol. 35, no. 1, pp. 1014–1021, Jan. 2020, doi: 10.1109/TPEL.2019.2912425.
- [23] H. Jbari, M. Haidoury, R. Askour, and B. Bououlid Idrissi, "Fuzzy logic controller for an EV's dual-source hybridization," *E3S Web of Conferences*, vol. 297, p. 01039, Sep. 2021, doi: 10.1051/e3sconf/202129701039.
- [24] H. Jbari, R. Askour, and B. B. Idrissi, "Real-time FPGA based simulator enabled Hardware-In-the-Loop for fuzzy control dual-sources HESS," *International Journal of Renewable Energy Research*, vol. 12, no. 2, pp. 880–891, 2022, doi: 10.20508/ijrer.v12i2.12922.g8472.
- [25] R. Morales-Caporal, O. Sandre-Hernandez, E. Bonilla-Huerta, J. C. Hernandez-Hernandez, and J. J. Hernandez-Mora, "DSP-based space vector modulation for a VSI-fed permanent magnet drive," in *2012 IEEE Ninth Electronics, Robotics and Automotive Mechanics Conference*, IEEE, Nov. 2012, pp. 261–266. doi: 10.1109/CERMA.2012.49.

BIOGRAPHIES OF AUTHORS






Hatim Jbari    was born in 1986 in Morocco. He is a Ph.D. and engineer in Electromechanical Engineering from ENSAM-Meknes, Morocco, and has a master degree of Engineering in Electric Vehicle and Mobility from Paris-Tech, France. His research interests are in the EMS algorithms, multi-physical modeling-control, and electric vehicle engineering. He can be contacted at email: ha.jbari@edu.umi.ac.ma.



Rachid Askour    was born in Casablanca-Morocco, he earned an engineering degree in 1996 from the ENSMR-Rabat, followed by a master's degree (DEA) in Electrical Engineering in 2002 from the Université des Sciences et Technologies de Lille, and a Ph.D. from ENSAM-Meknès in 2015. His research interests focus on power electronics, electric drives, and DSP-system control for electric vehicles. He has been working in the Electromechanical Engineering Department at ENSAM-Meknès since 1997. He can be contacted at email: r.askour@umi.ac.ma.



Badr Bououlid Idrissi    was born in Marrakech-Morocco, he earned an engineering degree from the ENSMR-Rabat in 1992, followed by a Ph.D. from the Faculté Polytechnique de Mons in Belgium in 1997. He is a professor at ENSAM-Meknès, Moulay Ismail University since 1999, with expertise in electrical machines and power electronics, his research is primarily dedicated to electric drives, DSP/FPGA based control for electric vehicles, and industrial control systems. He can be contacted at email: b.bououlid@umi.ac.ma.